◆ Human Brain Mapping 38:1815–1832 (2017) ◆

Cortical Thickness and Functional Connectivity Abnormality in Chronic Headache and Low Back Pain Patients

Qing Yang,[1] Zewei Wang,[2] Lixia Yang,[1] Yonghua Xu,[1] and Li Min Chen[1,3,4]*

[1]*Center for Biomedical Imaging Research, Shanghai Clinical Research Center/Xuhui Central Hospital, Chinese Academy of Sciences, People's Republic of China*
[2]*School of Mechatronic Engineering and Automation, Shanghai University, People's Republic of China*
[3]*Department of Radiology and Radiological Sciences, Vanderbilt University, Nashville, Tennessee*
[4]*Institute of Imaging Science, Vanderbilt University, Nashville, Tennessee*

Abstract: This study aims to characterize the psychological wellbeing of chronic headache (CH) patients, to identify cortical structural abnormalities and any associations of those abnormalities with resting state functional connectivity (rsFC), and to determine whether such rsFC abnormality is specific to CH patients. Compared with healthy controls (CON_{CH}), CH patients suffered from mild depression, sleep disturbances, and relatively poor quality of life. CH patients also exhibited widespread cortical thickness (CT) abnormalities in left premotor (BA6), right primary somatosensory (S1) and right prefrontal (BA10) cortices, as well as in regions of default mode and executive control networks. Using cortical regions with thickness abnormality as seeds, we found cortical region pairs showed strengthened rsFC in CH patients. Using the same seeds, rsFC analysis from chronic low back pain (CLBP) patients and their controls (CON_{CLBP}) identified abnormalities in non-overlapping cortical region pairs. Direct comparison of rsFC between CH and CLBP patients revealed significantly differences in thirteen cortical region pairs, including the four identified in CH and CON_{CH} comparison. Across all three groups (CH, CLBP and CON), the rsFC between left multisensory association area (BA39) and left posterior cingulate cortex (BA23) differed significantly. Eight regions showed CT abnormality in CLBP patients, two of which overlapped with those of CH patients. Our observations support the notion that CH and CLBP pain are pathological conditions, under which the brain develops distinct widespread structural and functional abnormalities. CH and CLBP groups share some similar structural abnormalities, but rsFC abnormalities in several cortical region pairs appear to be pathology-specific. *Hum Brain Mapp 38:1815–1832, 2017.*

Key words: cortical thickness; functional connectivity; chronic headache; chronic low back pain

Contract grant sponsor: "Strategic Priority Research Program (B)" of the Chinese Academy of Sciences, Brain Functional Connectivity Project; Contract grant number: XDB02010400.

*Correspondence to: Li Min Chen MD, PhD, Center of Biomedical Imaging Research, Shanghai Clinical Research Center/Xuhui Central Hospital, Chinese Academy of Sciences, 966 Mid HuaiHai Road, Shanghai, China. E-mail: lmchen@scrc.ac.cn OR Department of Radiology and Radiological Sciences, Institute of Imaging Science, Vanderbilt University Medical Center, AA 3115 MCN, 1161 21st Ave. S. Nashville 37027. E-mail: limin.chen@vanderbilt.edu

Received for publication 29 January 2016; Revised 11 November 2016; Accepted 22 November 2016.

DOI: 10.1002/hbm.23484
Published online 4 January 2017 in Wiley Online Library (wileyonlinelibrary.com).

INTRODUCTION

Chronic headache (CH) patients experience recurring pain and are at risk for psychological problems, such as depression, anxiety, and sleep disturbances. Patients living in chronic pain with psychological sequelae may need a multi-modal (e.g., pharmacological, psychological, and surgical) management strategy. Advances in noninvasive brain imaging techniques have associated pain perception with activations in specific brain regions and have revealed diverse gray and white matter structural abnormalities in patients with various chronic pain conditions. This has resulted in a greater recognition of the importance of supraspinal brain regions in the generation and maintenance of chronic pain states [Apkarian et al., 2013; Borsook et al., 2015; Davis and Moayedi, 2013; Mansour et al., 2014; Moayedi and Davis, 2013]. Nevertheless, controversy remains regarding the functional and behavioral relevance of structural brain abnormalities, such as alterations in cortical thickness (CT) (i.e., thickening vs. thinning), and the roles of particular cortical areas in different chronic pain conditions [Borsook et al., 2015; Davis and Moayedi, 2013; Emerson et al., 2014; Vincent et al., 2007]. Continuing developments in brain imaging paradigms may resolve these controversies, and perhaps elucidate structural and functional abnormalities on a circuit level. These advances would provide critical information about mechanisms, diagnostic and prognostic biomarkers, and putative therapeutic targets for chronic pain conditions.

The discovery of resting state functional connectivity (rsFC) networks on both large macro- and local mesoscales in humans and animals has revolutionized our understanding of the functional organization of both healthy and diseased brains [Biswal et al., 1995; Fox and Greicius, 2010; Freund et al., 2010; Ichesco et al., 2016; Kim et al., 2013; Sheline and Raichle, 2013]. Notably, brain regions that are engaged in the same functions or behaviors often exhibit strong functional connectivity at rest, as indicated by correlated fluctuations of low-frequency resting state functional MRI (rsfMRI) signals [Chen et al., 2011; Wang et al., 2013]. Brain regions with strong rsFC are usually connected anatomically [Vincent et al., 2007; Zhang et al., 2010]. Consequently, parcellation of functional circuits can be achieved through rsFC analysis [Mishra et al., 2014; Nelson et al., 2010].

Two observations motivated us to examine rsFC differences of cortical regions showing thickness abnormalities in chronic pain patients. First, correlated brain structure abnormalities (e.g., cortical thickness or volume), cortical function, and/or rsFC alterations have been discovered in several pathological conditions [Ceko et al., 2013; Jensen et al., 2013; Kong et al., 2013], including chronic pain [Apkarian, 2010; Hubbard et al., 2014]. Second, some of the cortical regions showing thickness abnormalities are known to be concurrently engaged in similar activities, such as pain perception and sensorimotor functions [Blankstein et al., 2010; Davis et al., 2008; Granziera et al., 2006; Moayedi et al., 2011]. We therefore started this study by asking: Do cortical regions that exhibit structural abnormality also exhibit functional connectivity alterations? We took a simple, hypothesis-driven, region of interest (ROI) based approach, and sought to identify and parcellate functionally connected regions and circuits among cortical regions that are involved in chronic pain states. Previous studies of CH have revealed compromised psychological wellbeing [Blackburn-Munro and Blackburn-Munro, 2001; Boakye et al., 2016] and have identified brain structural and functional abnormalities using MRI [Fasick et al., 2015]. However, questions remain as to whether abnormalities in brain structural and functional connectivity relate to each other and/or to psychological wellbeing, and if so, which specific brain regions are implicated. We propose that cortical regions exhibiting both structural and functional connectivity abnormalities in chronic pain conditions reflect a pathological abnormality underlying multifaceted chronic pain. To test this hypothesis, the present study focused on CH patients and addressed the following specific questions: (1) To what extent and in what aspect do CH patients suffer from compromised psychological wellbeing? (2) Do psychological measures correlate with the subjective pain magnitude? (3) Are there CH-related structural (CT) abnormalities, and if so, does it correlate with age and psychological measures? (4) Is cortical structural abnormality (CT) associated with rsFC abnormality, and if so, to what extent? (5) Do rsFC abnormalities differ between CH and chronic low back pain (CLBP) conditions? (6) Do CLBP patients exhibit similar CT abnormality as CH patients? (7) Do specific CT and rsFC abnormalities generalize across chronic pain patient groups?

MATERIALS AND METHODS

Participants

A total of 128 CH patients and age- and gender-matched controls (64 pairs) were recruited from outpatient headache clinics in the Shanghai Clinical Research Center/Xuhui Central Hospital, Chinese Academy of Sciences (Shanghai, China). Since white matter lesions have been consistently observed in CH patients and the general population [Kruit et al., 2004, 2010; Zheng et al., 2014] and the impact on CT and rsFC have not been well established, we used a participant exclusion criterion of greater than three white matter lesions in the present study. Twenty-five patients who met this criterion were excluded from the final data analysis. We found overall comparable prevalence of white matter lesions in both CH patient (37%) and control (32%) groups. Thus, 39 pairs of CH patients [10 men, 29 women; mean age ± standard deviation (SD), 43.4 ± 13.7 years] and their age- and gender-matched healthy controls (CON_{CH}; mean age ± SD, 44.0 ± 13.2 years) were studied. The CH group had a mean pain history of 14.0 ± 14.2 years (± SD; quartiles: 1.5, 7 and 23

years; minimum of three months). Based on criteria in the International Classification of Headache Disorders [ICHD-3, beta version, Headache Classification Committee of the International Headache Society (IHS), 2013], our CH group included 19 migraine headache, 10 tension-type headache, and 10 other primary headache participants.

A total of 124 CLBP patients and their age- and gender-matched controls (62 pairs) were recruited from outpatient clinics in Shanghai, China. Thirteen patients were excluded from the final data analysis because of more than three white matter lesions. We unexpectedly found high prevalence of white matter lesion in the CLBP (53%) and CON_{CLBP} (42%) groups. Thus, 49 CLBP patients (13 men, 36 women; mean age ± SD, 55.4 ± 9.4 years) and their age- and gender-matched healthy controls (CON_{CLBP}; mean age ± SD, 55.2 ± 9.3 years) were included in the final analysis and quantification. The CLBP group had a mean pain history of 6.4 ± 8.3 years (± SD; quartiles: 2, 4 and 7.4 years; minimum of 3 months). Chinese versions of Nordic Musculoskeletal and Roland-Morris Questionnaires, as well as physical examinations, were used to classify CLBP patients [Takekawa et al., 2015; Yi et al., 2012]. Using the CLBP classification criteria described by Chou and colleagues [Chou et al., 2007], included CLBP patients were classified into three main categories: nonspecific (71.4%, 35/49), pain associated with radiculopathy (with the presence of sciatica, neuropathic; 28.6%, 14/49), and other spinal pathology (secondary to known disease, such as tumor or inflammation; 0/49).

All participants were of the Han Chinese ethnicity. Each participant provided written consent for participating and acknowledged that s/he had been informed about the purpose of the study. Our research complied with the Code of Ethics of the World Medical Association (Declaration of Helsinki) and NIH guidelines on research performed on human subjects. This study was approved by the Institutional Review Board of the Shanghai Clinical Research Center/Xuhui Central Hospital, Chinese Academy of Sciences.

Questionnaires

Before the participants underwent an MRI scan, data were collected via a pre-imaging questionnaire packet that included the following components: (1) a general demographic and medical history (including condition duration) survey, (2) the IHS diagnostic questionnaire (CH group only); (3) the Short-Form Health Survey [SF-36; Ware and Sherbourne, 1992]; (4) the Beck Depression Inventory [BDI; Beck and Alford, 2009]; (5) the Pittsburgh Sleep Quality Index [PSQI; Buysse et al., 1989]; (6) the State-Trait Anxiety Inventory [STAI; Tilton, 2008]; and (7) the Hamilton Rating Scale for Depression [HRSD; Hamilton, 1960; Williams, 1988]. Each patient was also instructed to report his/her magnitude of pain on a numeric 0–10 rating scale at the time the questionnaire was completed, anchored by ratings of no pain to strongest pain imaginable, respectively.

The SF-36 evaluates overall health status (i.e., vitality, physical functioning, bodily pain, general health perceptions, physical, emotional role functioning, social role functioning, and mental health), with a lower score indicating a lower quality of life. The BDI is a self-report inventory that rates severity of depression symptoms on affective and somatic subscales, with higher scores indicating greater severity of depression. The HRSD is a structured interview scale that assesses depression level based on symptoms such as depressed mood, guilty feelings, suicidal ideation, sleeping disturbances, anxiety, and weight loss, with a higher score indicating more severe depression. Both scales are used to fully characterize the severity of depression. The PSQI assesses sleep quality (i.e., subjective sleep quality, sleep latency, sleep duration, habitual sleep efficiency, sleep disturbances, use of sleeping medication, and daytime dysfunction), with a higher PSQI value indicating greater difficulty in sleeping. The STAI assesses both state anxiety (i.e., anxiety about an event) and trait anxiety (i.e., anxiety level as a personal characteristic), with higher scores indicating higher levels of anxiety.

MRI Data Acquisition

All participants were scanned in a 3-T Siemens MRI system (Magnetom Verio) with a 32-channel head coil. T1-weighted structural images were acquired with a three-dimensional (3D) magnetization-prepared rapid gradient-echo (MP-RAGE) sequence (echo time = 2.98 ms, repetition time = 2,530 ms, acquisition matrix = 224 × 256 × 192, isometric voxel size = 1 × 1 × 1 mm^3). T2*-weighted rsfMRI series were acquired with an echo-planar imaging sequence (echo time = 30 ms, repetition time = 2,000 ms, acquisition matrix = 64 × 64, in-plane resolution = 3 × 3 mm^2, slice thickness = 5 mm). For each participant, 28 axial image slices without gaps were obtained in an interleaved-ascending manner covering the entire brain, and rsfMRI data (300 volumes, 10 minutes duration) were collected.

MRI Data Analysis

Structural MRI analysis

FreeSurfer software (https://surfer.nmr.mgh.harvard.edu/) was used for image preprocessing and for quantifying whole-brain CT differences between paired groups. For the raw MP-RAGE structural images of each participant, we performed motion correction, Talairach registration, intensity correction, brain extraction, and normalization based on a Gaussian Classifier Atlas. The resulting volumes were used to segment white matter and the gray–white matter interface to estimate CT. Manual manipulations (i.e., adjusting Talairach registration and adding points for gray-matter separation)

TABLE I. Cortical regions with CH-associated thickness changes (Fig. 2) [Color table can be viewed at wileyonlinelibrary.com]

Index	DK atlas	BA	*t* value	Coordinates (*x*,*y*,*z*)			Size (mm^2)
° 1	L medial orbitofrontal cortex	L anterior cingulate cortex (ACC) (BA24)	4.5212	−6.4	16.0	−16.2	126.43
2	L inferior parietal cortex	L multisensory association area (BA39)	2.4505	−39.6	−68.2	44.9	100.93
° 3	L precentral gyrus	L premotor cortex (BA6)	−2.4185	−48.7	−1.7	40.6	229.64
° 4	L posterior cingulate cortex (PCC)	L PCC (BA23)	2.7635	−4.0	−12.6	33.1	282.06
5	L middle temporal gyrus	L multimodal posterior area (BA21)	−2.4923	−59.0	−15.1	−23.8	164.05
° 6	L lingual gyrus	L visual association area (BA18)	−2.4268	−25.1	−64.0	1.1	225.26
° 7	R rostral middle frontal gyrus	R prefrontal cortex (BA10)	−2.8411	22.7	56.4	16.2	271.50
° 8	R superior parietal cortex	R secondary sensorimotor cortex (BA7)	−3.5559	33.5	−44.7	48.9	112.13
9	R inferior parietal cortex	R multisensory association area (B39)	2.3254	47.6	−53.8	33.2	122.50
10	R postcentral gyrus	R primary somatosensory cortex (S1)	2.7027	5.4	−38.1	74.0	141.30
° 11	R lateral occipital cortex	R secondary visual cortex (V2)	−2.9200	30.0	−80.8	−9.1	421.42
° 12	R cuneus cortex	R primary visual cortex (V1)	−2.8644	10.1	−69.3	17.9	328.96

Note: "°" indicates regions survived the multiple comparison corrections (Monte Carlo simulation, $P < 0.05$, FreeSurfer). Regions in left (L) or right (or R) hemispheres are highlighted by blue or red background, respectively. *x*-*y*-*z* coordinates are in MNI space. Positive and negative numbers indicate cortical thickening and thinning in CH patients, respectively.

were used to improve gray matter parcellation accuracy and CT quantification. For group analysis, we used the Freesurfer Qdec tool to average morphometric data across subjects. Surface-based smoothing with a full-width at half-maximum (FWHM) of 10 mm was applied. Finally, we assessed CT differences between CH versus CON_{CH} groups using two-sample two-tailed *t*-tests without multiple comparison correction. To indicate the confidence level of a CT difference, regions that survived Monte Carlo correction were labeled in Tables I and III with Montreal Neurological Institute (MNI) coordinates of the cortex showing the largest significant value in each region. Cortical regions found to have significant group differences (satisfying threshold $P < 0.05$, peak threshold of $P < 0.01$ and cluster size ≥ 60 mm^2) in CT were overlaid on inflated brain surfaces [Desikan/Killiany (DK) atlas; Desikan et al., 2006] for display (see Fig. 2). To link DK atlas (used by FreeSurfer) defined cortical regions to the known neuroanatomical regions (e.g., postcentral gyrus: primary somatosensory cortex), we included the corresponding readouts as Brodmann Areas (BA) using free online "MNI<->Talairach with Brodmann" software (http://sprout022.sprout.yale.edu/mni2tal/mni2tal.html) in our data reports. To determine the main functions of each BA, we referenced the information summarized in the free online "Brodmann's Interactive Atlas 1.1" (www.fmriconsulting.com/brodmann/index.html) in Tables I and III. These cortical regions were used as seed ROIs in the subsequent rsFC analysis.

Correlation analysis between CT and psychometrics

To understand the relationship of CT measures with age, pain rating, and psychological scores, we generated scatter plots of different measures (i.e., CT and age) across all subjects (i.e., CH and CON_{CH}), and performed linear regression and a Pearson's correlation analysis. The slope of the linear fit line (b1), correlation *r*-values, and statistical *P*-values were evaluated (e.g., Figs. 3 and 4).

RsfMRI analysis

Seed ROI-based rsfMRI data analysis was performed with a custom toolbox in Statistical Parametric Mapping software, version 8 (SPM8, http://www.fil.ion.ucl.ac.uk/spm/). Preprocessing steps included: the removal of the first 10 image volumes, slice time correction for interleaved acquisitions, within subject 3D motion correction of image time series, within subject co-registration of the rsfMRI and structural MRI images with rigid-body transformation, normalization via registering source images to a software-provided template, and spatial smoothing by convolving image volumes with a Gaussian kernel (FWHM = 6 mm) in SPM8. RsfMRI signals were band pass filtered (0.01–0.08 Hz). The 3D motional parameters were regressed out as nuisance signals. We did not observe statistically different motion noise between CH and CON_{CH} groups, nor did we observe significant correlations between the age and the motion parameters in both CH and CON_{CH} groups (see the time plots and quantification in Supporting Information Fig. 1). Segmented white matter and CSF masks in SPM were used to extract the RsfMRI signal time courses of white matter and CSF voxels. PCA (principle component analysis) components accounting for 70% of the variance in white matter and CSF signals were used as nuisance signals for regression analysis with custom Matlab scripts.

Inter-regional correlation coefficients were quantified to evaluate differences in rsFC strength (i.e., enhanced or weakened) between pre-defined ROI seeds. Seed locations were defined by the trilinear coordinates of the cortical regions in the MNI space that showed the greatest

significant CT abnormality. Each seed was spherical with a 10-mm radius; rsfMRI signal time series from all voxels within each ROI were extracted for analysis. A pairwise correlation coefficient (r-value) was calculated for each ROI pair combination to indicate the strength of inter-regional rsFC. Two-sample two-tailed t-tests adjusted for multiple comparisons using Benjamini–Hochberg false discovery rate (FDR = 0.05) correction were used to compare the rsFC strength differences between groups, with $P < 0.05$ being considered statistically significant.

Functional connectivity map generation

We used BrainNet Viewer [Xia et al., 2013] to summarize and display the cortical structural and functional connectivity abnormalities in a 3D whole-brain platform. Mean correlation values of pre-defined ROI pairs were selected and rearranged as the inputs for BrainNet Viewer (MATLAB toolbox). BrainNet Viewer provides enhanced visualization of the mean correlation levels of the ROI pairs. We used the template "surface" file ICBM152 as the underlying 3D structural image, and then applied the information (e.g., coordinates, labels, colors, etc.) from the pre-defined ROI seeds to form the "node" file. The trilinear coordinates of the ROI seeds, which yielded CT abnormality between the CH and CON_{CH} groups (Fig. 6C), were input as nodes for the 3D visualization. Nodes residing at close distances, as measured by their coordinates, were coded with similar colors and re-grouped together. The ROI pairs (nodes) showing significantly altered rsFC were linked with lines whose weights represent correlation strength, such that thicker lines indicate greater group differences in rsFC.

RESULTS

Psychometrics

The mean psychometric results for the questionnaires completed by the CH and CON_{CH} groups are reported in Supporting Information Table. Briefly, SF-36, BDI, PSQI, and HRSD scores differed significantly between the two groups ($P < 0.05$). Relative to the CON_{CH} group, the CH group had a lower overall quality of life, along with more fatigue problems, sleep disturbances, and depression symptoms. The CH group also displayed slightly more anxiety. The distribution of scores relative to diagnostic criteria is shown in Figure 1A. The average pain rating of our CH cohort was 6.2 ± 2.2 (mean $\pm$ SD; quartiles: 4, 6, and 8). Interestingly, we found relationships between the psychological scores and the subjective pain ratings (Fig. 1B). Patients with more pain tended to be less healthy overall than those with less pain: those with more pain experienced more fatigue, sleep disturbance, and depression, but interestingly experienced less anxiety. Statistically, however, the trends were not significant, indicating a large variability in the severity of symptoms across CH patients and pain ratings.

CT Abnormality in CH Patients

Compared with the CON_{CH} group, the CH group had widespread gray matter thickening or thinning in numerous cortical areas: left medial orbitofrontal cortex [left anterior cingulate cortex (ACC, BA24)], bilateral inferior parietal cortex [bilateral multisensory association area (BA39)], left precentral gyrus [left premotor cortex (BA6)], left posterior cingulate cortex [left PCC (BA23)], left middle temporal gyrus [left multimodal posterior area (BA21)], left lingual gyrus [left visual association areas (BA18)], right rostral middle frontal gyrus [right prefrontal cortex (BA10)], right superior parietal cortex [right secondary sensorimotor cortex (BA7)], right postcentral gyrus [right primary somatosensory cortex (S1)], right lateral occipital cortex [right secondary visual cortex (V2)], and right cuneus cortex [right primary visual cortex (V1)] (Fig. 2 and Table I). The thickness abnormalities were generally asymmetric, though a bilateral change in the multisensory association area (within inferior parietal cortex) was observed. Several pain-related cortical regions, including the ACC (a medial orbitofrontal region that is engaged in emotional, motivational and executive functions), premotor cortex, S1 cortex, and PCC regions showed considerable abnormalities (regions surviving multiple comparison correction are labeled in Table I). Of twelve identified regions with significant CT abnormality, five regions [left ACC (BA24), left PCC (BA23), bilateral multisensory association area (BA39) and right S1 cortex in Fig. 2] showed thickening, while seven regions [left premotor cortex (BA6), left multimodal posterior area (BA21), left visual association area (BA19), right prefrontal cortex (BA10), right secondary sensorimotor cortex (BA7), right V1 and V2 cortices] exhibited thinning. The cortical locations, peak statistical significances (t values), MNI coordinates, and cluster sizes of all 12 of these regions are reported in Table I. Notably, 8 of the 12 regions exhibited a higher level of statistical confidence (i.e., survived multiple comparison correction) in CT differences between the two groups. Box plots of the distributions of the CT measures of five representative cortical ROIs regions are shown in Figure 3B, D, F, H, and J.

Distribution of CT as a Function of Age

We then directly compared CT abnormality as a function of age to determine whether CH patients are at higher risk for CT abnormalities. With increases in age and relative to CON_{CH} group measurements, the CH group showed significant thinning in left PCC ($P = 0.03$, cluster 4), the left multimodal posterior (middle temporal gyrus, $P = 0.02$, cluster 5) and left visual association (lingual gyrus, $P = 0.05$, cluster 6) areas (red lines in Fig. 3D, F,

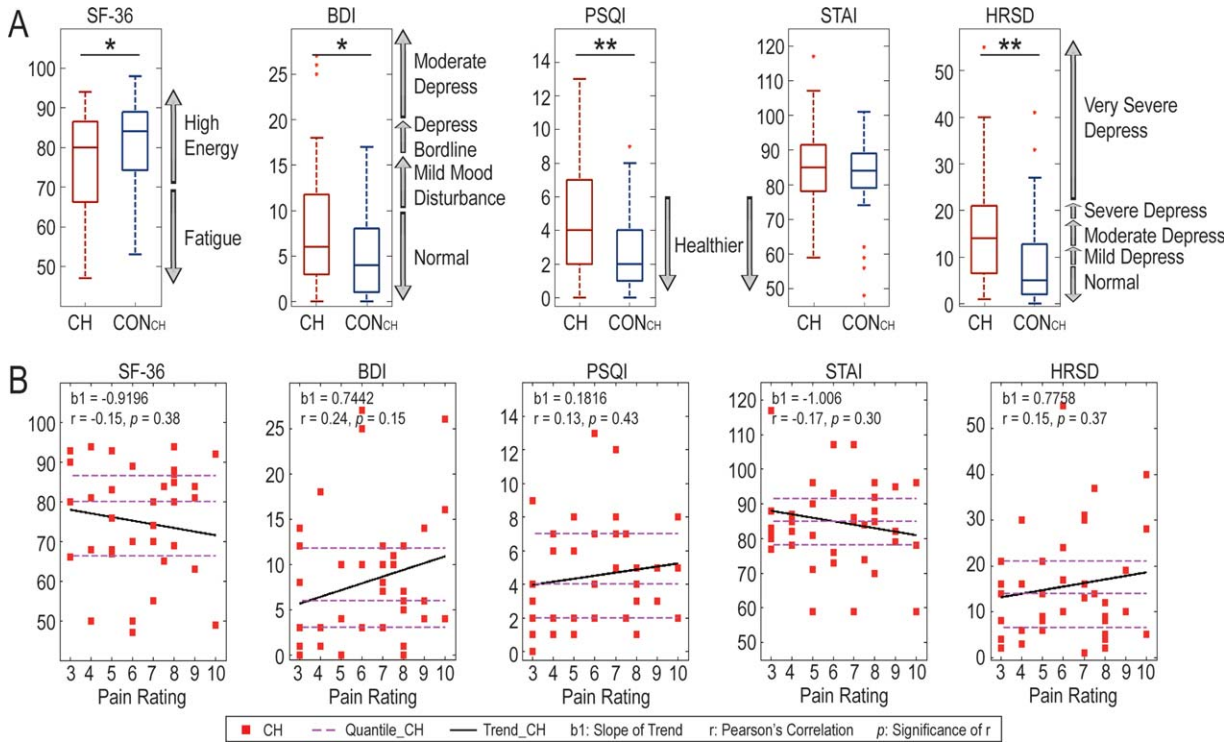

Figure 1.

Statistical distribution of psychometric results for the CH and CON_{CH} groups (Supporting Information Table) and the correlations between psychometric scores and pain ratings for CH patients. (A) Box plots of psychometric results with their diagnostic criteria (gray arrows on the right side of box) of the patients (red boxes) and controls (blue boxes). $^{*}P < 0.05$; $^{**}P < 0.01$. (B) Scatter plots of psychometric measures as a function of self-reported subjective pain ratings (0–10 scale) in CH patients. Thick black lines: linear regression results with the slope b1; dashed magenta lines: quartiles on the vertical axis. [Color figure can be viewed at wileyonlinelibrary.com]

and H). For the CON_{CH} group, we observed no correlations of CT changes with increases of age in the above mentioned regions, with the exception of one temporal region (multimodal posterior area) that showed a thinning trend (Fig. 3F). The most pronounced age-associated CH group-specific change was thinning in the left multimodal posterior area (0.3 mm, Fig. 3D).

Relationships Between Regional CT Measures and Psychological Scores in Both CH and CON_{CH} Groups

Since the regions showing both abnormal structural and functional connectivity are very likely among those most severely affected brain regions during the course of chronic pain, we plotted CT measures as a function of the different psychological scores for the five ROIs showing significantly different rsFC between CH patients and CON_{CH} groups (Fig. 4) to understand whether CT correlates with psychological wellbeing and/or pain rating in both patients and their controls. In all five ROIs, CT showed no relationship with the pain ratings in CH patients (see the last column in Fig. 4). Across all five ROIs and psychological measures, there were no strong correlations shared between CH and CON_{CH} groups. For CON_{CH}, significant inverse correlations between CT and SF-36 scores were detected in the left multisensory association and right S1 regions (first column in Fig. 4A, E), indicating normal subjects with a higher quality of life and less fatigue exhibited thinning in these cortices. The CT of the left multisensory association area also showed an inverse correlation with sleep disturbance scores (PSQI), but this did not reach a level of significance ($P = 0.09$; third panel in Fig. 4C). For CH, the CT of the left visual association area showed significant inverse correlation ($P = 0.03$) with the PSQI and trending ($P = 0.06$) positive correlation with anxiety scores (SATI; third and fourth panels in Fig. 4D). The CT of the left multisensory association area also showed strong, but not significant ($P = 0.07$), inverse correlation with the depression score (HRSD; fifth column in Fig. 4C).

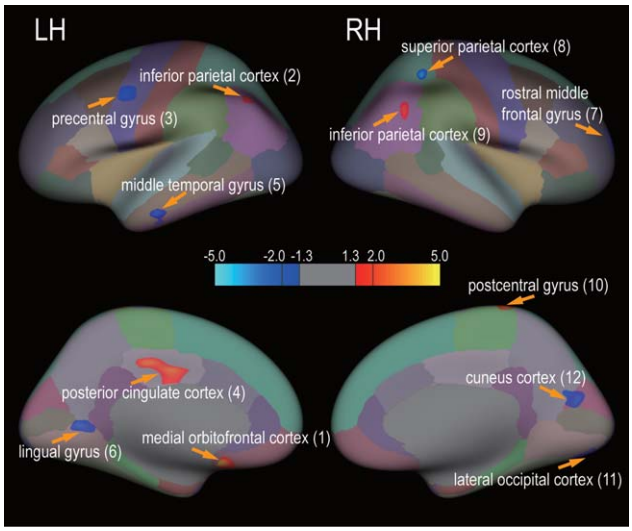

Figure 2.

Widely distributed CT abnormality in CH relative to CON_{CH} groups (39 pairs). Cortical regions that exhibited thickness abnormality are illustrated on an inflated, parcellated brain surface (color coded for 64 cortical areas, DK atlas). Light blue-blue and yellow-red colors indicate thickening and thinning, respectively. Horizontal color bar shows the range of CT abnormality (*t*-values). Thickness abnormality (two-sample two-tailed *t*-test) was thresholded at $P < 0.05$ ($|t| > 1.3$), peak significant value $P < 0.01$ ($|t| > 2$), and minimal cluster size of 60 mm^2. Patches are numbered from left (L) to right (R) hemispheres.

RsFC Between Regions Showing Abnormal CT in CH Patients

Matrix plots (Fig. 5) of average Pearson's inter-regional correlations of rsFC between all possible combinations of the twelve ROIs with CH-associated structural abnormality (Table I) for the CH and CON_{CH} groups revealed several interesting features. First, inter-regional connectivity strengths were generally stronger for the CH group than for the CON_{CH} group (mean $r = 0.52$ vs. $r = 0.47$, respectively), as illustrated by the number of high-correlation pixels (red-orange) in Figure 5A,B. Second, only 6 of the 10 ROIs showing the strongest correlations in each group were shared between the two groups (Fig. 5C,D), including a right secondary sensorimotor cortex correlation with the right S1 cortex and a left PCC correlation with the right V1 cortex (dark red pixels in Fig. 5C,D). A strong connection between the left multisensory association areas and left PCC ($r = 0.68$) was only present in the CH group, whereas a strong connection between premotor and S1 cortices was only observed in the CON_{CH} group. Third, there were no consistent relationships between rsFC strength and CT change direction (i.e., thickening or thinning). That is, strong rsFCs did not show a preference for the nature of thickness abnormality; they occurred between thickened regions, between thickened and thinned regions, and between thinned regions.

Comparison of group-averaged correlation coefficients of each ROI pair revealed significantly different correlation strengths ($P < 0.05$, two-sample double-tailed *t*-test, Fig. 6A,B) in four ROI pairs (among five ROI regions) between the two groups, with the CH group exhibiting stronger rsFC correlations in all four of these comparisons. Four of the five regions involved (clusters 2, 4, 5, and 6 in Fig. 2) were located in the left hemisphere, whereas only one (cluster 10 in Fig. 2) was located in the right hemisphere. The left multisensory association area (cluster 2) appeared to be a hub of the altered rsFC network in CH patients, which included: the left multisensory association area–left PCC (2–4), the left multisensory association area–left multimodal posterior area (2–5), the left multisensory association area–left visual association area (2–6), and the left multisensory association area–right S1 cortex (2–10) relationships. A 3D whole-brain visual representation of the distributed cortical network exhibiting significant thickness (color-coded nodes) and rsFC abnormality (line-connected nodes) in the CH group is shown in Figure 6C.

Because our CH patient population is heterogeneous, we then evaluated whether data of any one sub-group biased the population results. The matrix plots of the pair-wise correlation analysis of different sub-group patients (i.e., migraine, tension type, or others) and their controls showed that population results were not driven by any one of the sub-groups (see Supporting Information Fig. 2). Only one ROI pair (the left multisensory association area and left PCC) showed a significant strengthened rsFC difference in the migraine group (compare Supporting Information Fig. 2A,B).

RsFC Abnormality in CLBP Patients

To determine whether CLBP patients share similar rsFC abnormalities between brain regions exhibiting CT abnormality in CH patients, we used the 12 ROIs identified in CH versus CON_{CH} comparisons as the seeds to quantify the rsFC in three group comparisons: (1) between CLBP and CON_{CLBP} groups, (2) between CH and CLBP groups, and (3) between CON_{CH} and CON_{CLBP} groups. We observed generally similar inter-regional rsFC patterns in the CLBP group, relative to the CH group, for the aforementioned set of 12 ROI pairs (compare Fig. 7A,B with Fig. 5A,B). The 10 ROI pairs with the strongest rsFC in the CLBP group are plotted in Figure 7C,D. Strong inter-regional correlations for the left multisensory association area–right S1 cortex and the left PCC–right V1 cortex region pairs were identified in both CH and CLBP patients (see dark red pixels with diamonds in Fig. 7C,D). Interestingly, two ROI pairs (left multisensory association area–left PCC, and left premotor cortex–left PCC) showed stronger rsFC in the CLBP patients than in CON_{CLBP}, whereas two others (left premotor cortex–right V1 cortex, and right multisensory association area–right V1 cortex) exhibited

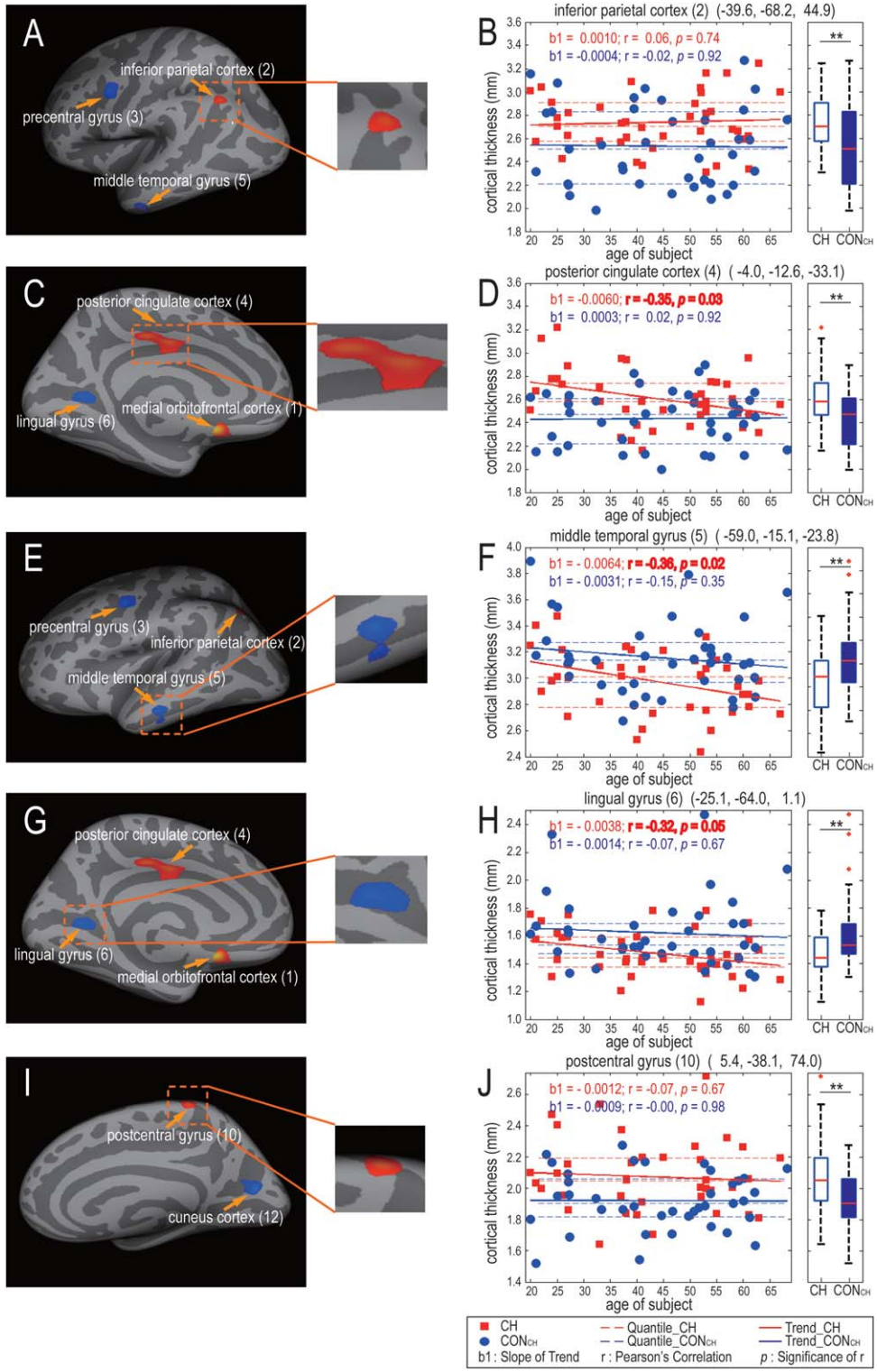

Figure 3.

Distribution of CT measurements as a function of age in CH and CON_{CH} groups for five representative regions. (A, C, E, G, I) Inflated brain surface maps show the location and size of regions with thickness abnormality. Inserts in the middle column show zoomed-in views of these regions. (B, D, F, H, J). Scatter (left) and box (right) plots of CT distributions in left inferior parietal cortex (2), left PCC (4), left middle temporal gyrus (5), left lingual gyrus (6), and right postcentral gyrus (10) for both groups. Solid lines represent linear regression with the slope b1; dotted lines indicate quartiles. The Pearson's correlations between CT and age are also shown (*r* and *p* values). The CT of PCC (4), middle temporal gyrus (5) and lingual gyrus (6) in CH patients decreases with increasing age ($P < 0.05$). In the box plots, red lines indicate median values; top and bottom blue lines indicate 75% and 25% quartiles; error bars (whiskers) show SDs; outliers are plotted as red crosses. ** $P < 0.01$. [Color figure can be viewed at wileyonlinelibrary.com]

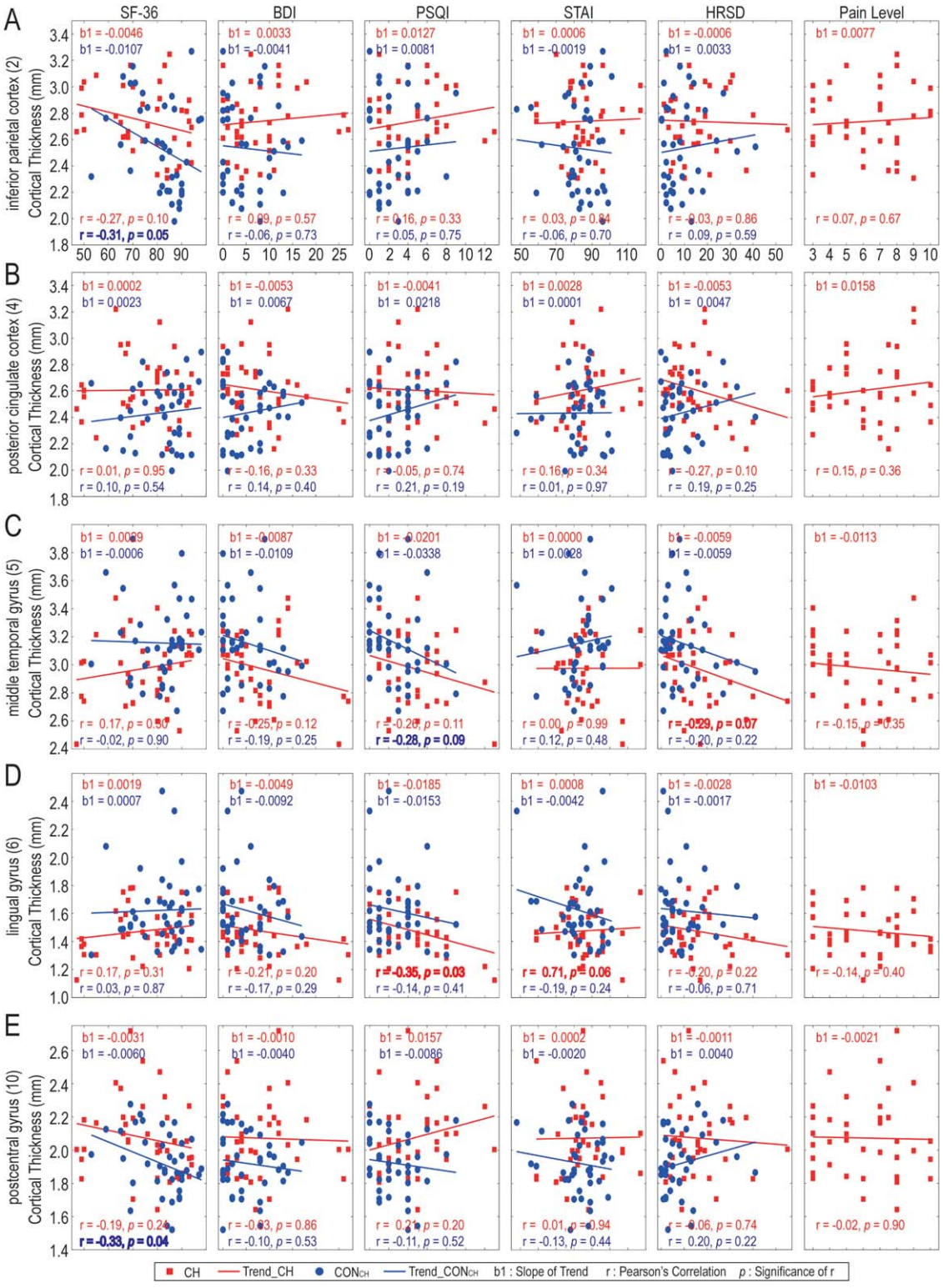

Figure 4.

CT of five ROIs distributed with psychometric results (SF-36, BDI, PSQI, STAI, HRSD) of CH and CON_{CH} and pain rating of CH patients. Red and blue lines represent linear regression of patient and control groups with the slope b1. The Pearson's correlations (*r* and *P*) of CT and questionnaires are also shown. The CT of left lingual gyrus (6) [left visual association area (BA18)] in patients decreases with increasing PSQI scores ($P < 0.05$); and the CT of left inferior parietal cortex (2) [left multisensory association area (BA39)] and right postcentral gyrus (10) (right S1 cortex) in controls decreases with increasing SF-36 scores ($P < 0.05$). [Color figure can be viewed at wileyonlinelibrary.com]

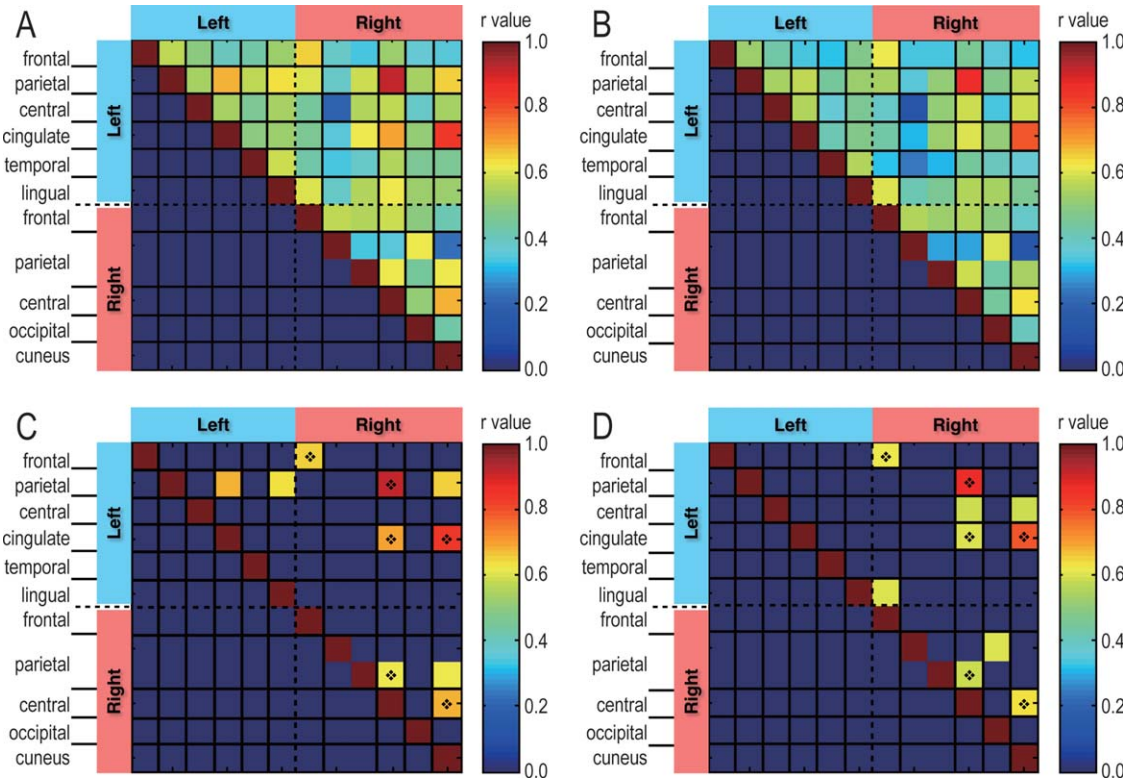

Figure 5.

Pairwise rsFC between cortical regions showing thickness abnormality between CH and CON_{CH} groups. Matrix plots of mean rsFC in (A) CH and (B) CON_{CH} with their top 10 values shown, respectively, in (C) and (D). The dark diamond indicates ROI pairs shown strong rsFC (CH: $r > 0.62$; CON_{CH}: $r > 0.59$) in both groups.

stronger rsFC in the CON_{CLBP} than in CLBP patients (pixels without diamonds in Fig. 7C,D). Two ROI pairs (left premotor cortex–right V1 cortex and right V2 cortex–right V1 cortex) showed significantly weakened rsFC ($P < 0.05$) in CLBP patients compared with the CON_{CLBP} group (Fig. 7E,F).

Direct comparisons of inter-regional rsFC between CH versus CLBP groups identified significantly different rsFC in thirteen ROI pairs (CH > CLBP), which did not overlap with the two ROI pairs (left premotor cortex–-right V1 cortex and right V2 cortex–right V1 cortex) detected between the CLBP and CON_{CLBP} comparison (compare Fig. 8A with Fig. 7E). We also computed rsFC differences between the two control groups (CON_{CH} vs. CON_{CLBP}) as a test of the representativeness of our controls, and found that there was only one region [left ACC (an emotional/motivational/executive function region)–left visual association area] that showed a difference (Fig. 8B).

In summary, pair-wise inter-regional rsFC analysis revealed that different groups (CH vs. CON_{CH}, CLBP vs. CON_{CLBP}, CH vs. CLBP, CON_{CH} vs. CON_{CLBP}) exhibited significantly different inter-regional rsFC in unique sets of ROI pairs (Table II). ROI pairs showing abnormal rsFCs in the CH versus CON_{CH} comparison did not overlap with those in the CLBP versus CON_{CLBP} comparison. Four ROI pairs showed strengthened rsFC in both the CH versus CON_{CH} and CH versus CLBP comparisons. Only one ROI pair (left multisensory association area–left PCC) showed significant difference among all three groups (CN, CLBP, $CON_{CH+CLBP}$; $P < 0.05$, one-way ANOVA).

CT Abnormality in CLBP Patients

Lastly, to understand the association between CT abnormalities in different chronic pain conditions, we quantified the CT differences between the CLBP and CON_{CLBP} groups (Fig. 9), and then compared these differences with those identified in the CH versus CON_{CH} comparison. We found that the CLBP group exhibited widely distributed CT abnormalities in eight cortical regions, of which two overlapped with those of the CH group (region pairs surviving multiple comparison correction are labeled in Tables I and III). These regions included: the left inferior

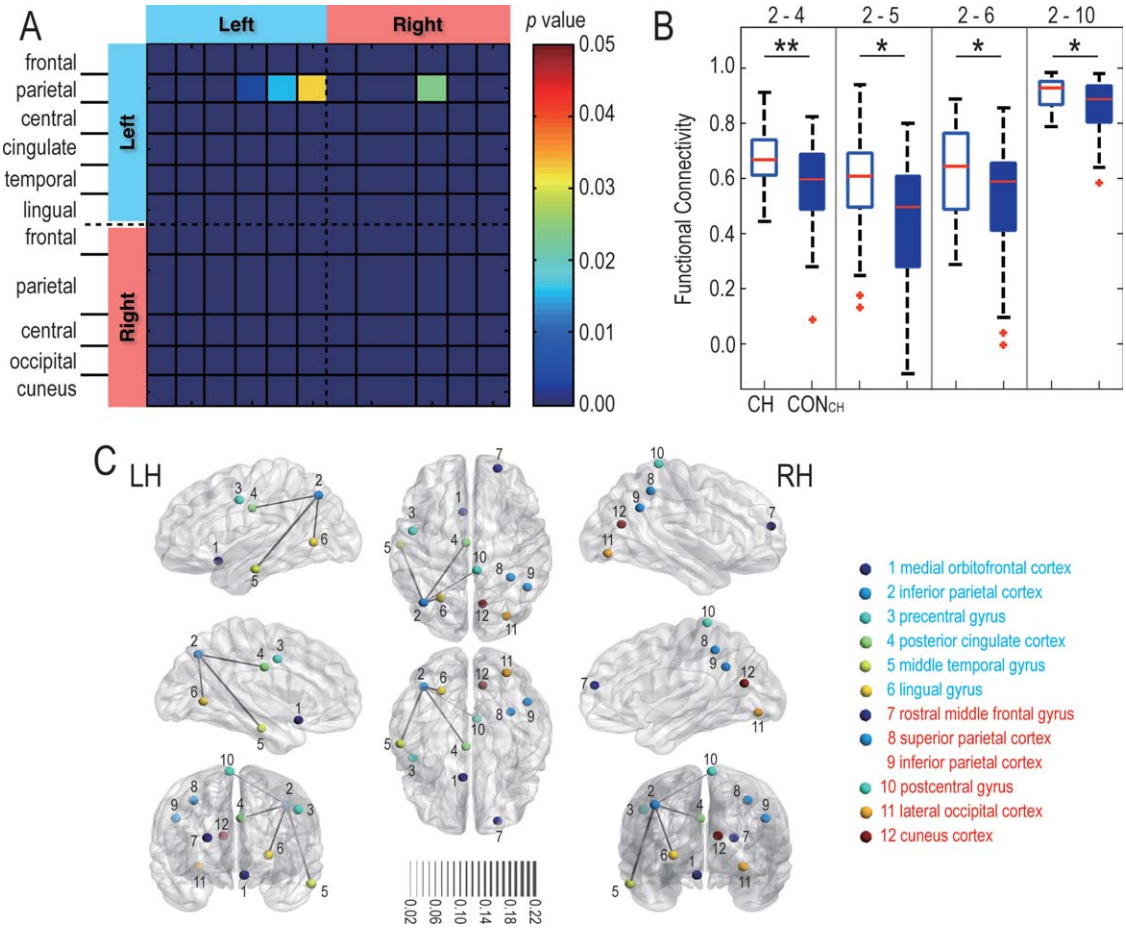

Figure 6.

Matrix plots and 3D visualization of ROI pairs with rsFC differences between CH and CON_{CH} groups. (A) Four ROI pairs with significant group difference in rsFC. (B) Box plots of rsFC distributions for each group for those four ROI pairs. Red lines indicate medians; top and bottom blue lines indicate 75% and 25% quartiles; error bars (whiskers) show SDs; outliers are plotted as red crosses. $^{*}P < 0.05$; $^{**}P < 0.01$. (C) Colored nodes represent ROI seeds with same color scheme representing ROIs within the same lobe (e.g., frontal and parietal cortices). Internodal lines are weighted to reflect magnitude of mean correlation coefficient values between the groups. The four ROI pairs (2–4, 2–6, 2–5, and 2–10) with significant differences in correlation coefficients between the two groups (Fig. 6A) are linked with lines. LH and RH: left and right hemispheres. [Color figure can be viewed at wileyonlinelibrary.com]

parietal cortex [left multisensory association area (BA39)], left precentral gyrus [left premotor cortex (BA6)], left PCC (BA31), left middle temporal gyrus [left multimodal posterior area (BA21)], right rostral middle frontal gyrus [right prefrontal cortex (BA9)], right superior parietal cortex [right secondary sensorimotor cortex (BA7)] and right precentral gyrus [right primary motor cortex (M1, BA4)]. When taking into account the confidence level of the CT measure differences by looking at the regions that survived the multiple comparison correction, the only two regions showing robust cortical thickness abnormality in both CH and CLBP conditions are the left PCC and right rostral middle frontal gyrus (right prefrontal cortex).

DISCUSSION

In the present study, we found that our group of CH patients were suffering from mild depression and sleep disturbances, and had a lower quality of life than their demographically matched controls. They also exhibited diverse CT abnormality, in core pain regions, such as the premotor and S1 cortices, PCC, and regions in the default mode network (DMN). RsFC analysis of rsfMRI data for ROIs selected based on CT findings revealed four ROI pairs (among five regions) with altered rsFC in CH patients, and only two such pairs in the CLBP group. Compared with the rsFC of the CH group, CLBP patients exhibited significant

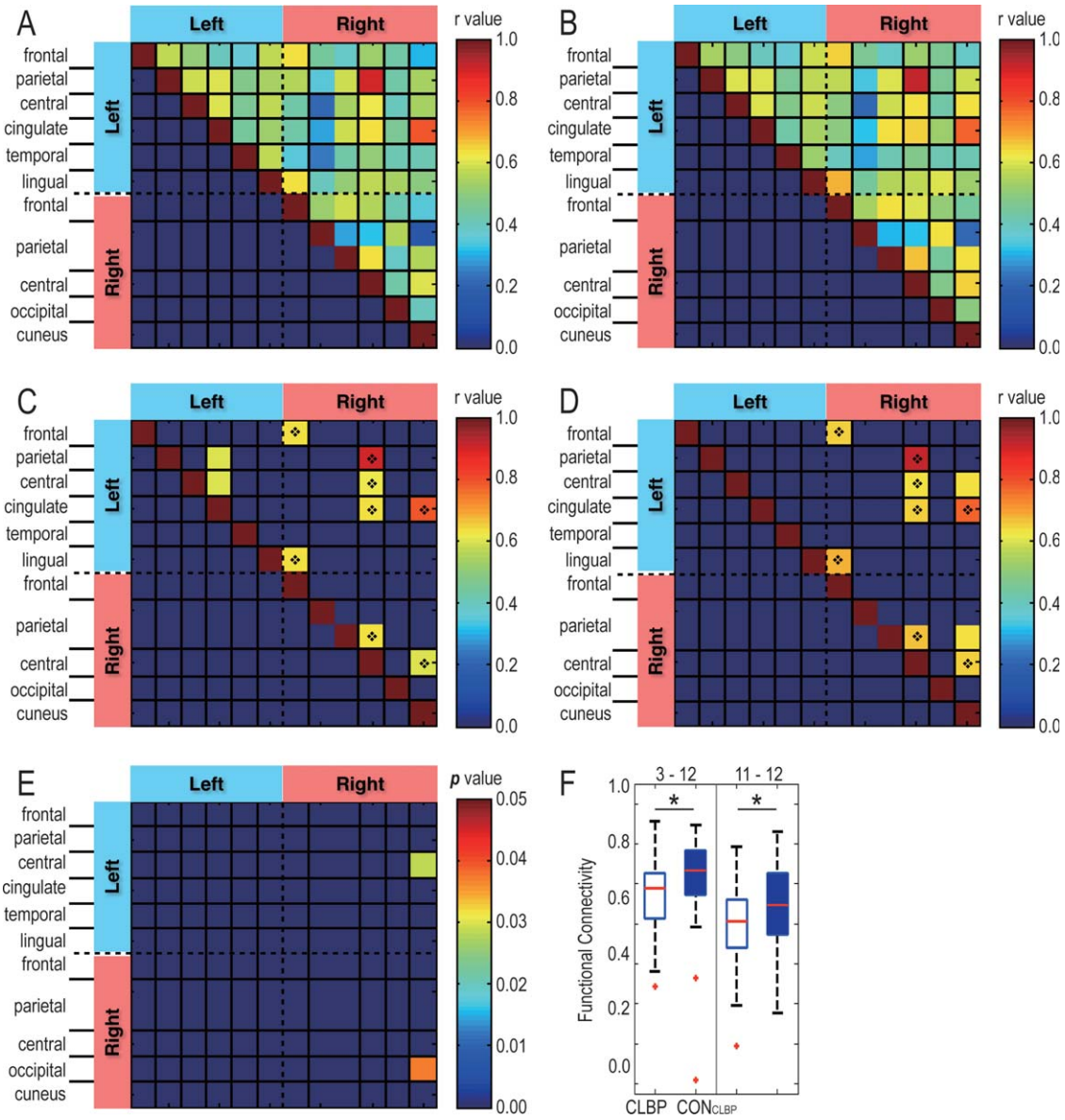

Figure 7.

Pairwise rsFC between CLBP patients and their controls CON_{CLBP} (49 pairs) using the same ROI seeds as in Fig. 6. Matrix plots of mean rsFC in (A) CLBP and (B) CON_{CLBP} with their top 10 values shown, respectively, in (C) and (D). Shared pixels are indicated by the diamond. (E) rsFC of left precentral gyrus (left premotor cortex) – right cuneus cortex (right V1 cortex) (3–12) and right lateral occipital cortex (right V2 cortex) – right cuneus cortex (right V1 cortex) (11–12) differed between the two groups. (F) Box plots of the group FC (*r* value) distributions for ROI pairs of 3–12 and 11–12. Red lines indicate medians; top and bottom blue lines indicate 75% and 25% quartiles; error bars (whiskers) show SDs; outliers are plotted as red crosses. $^*P < 0.05$, two-sample double-tailed *t*-test. [Color figure can be viewed at wileyonlinelibrary.com]

rsFC strength differences in partially overlapping and unique sets of ROI pairs. These observations support the notion that CH pain is a pathological condition characterized by structural and functional abnormality, and suggest that rsFC alterations in some cortical regions do not generalize across different chronic pain conditions.

Compromised Psychological Wellbeing of CH Patients

CH patients' scores on five psychometric instruments suggested that they had compromised psychological wellbeing characterized by fatigue (SF-36), depression

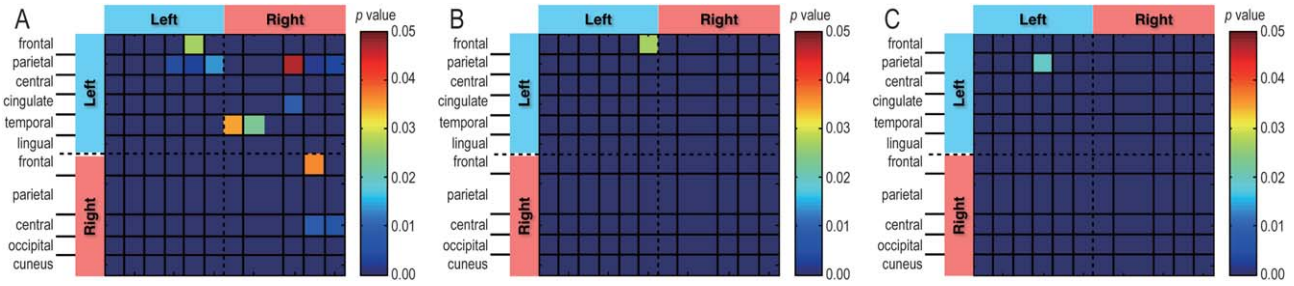

Figure 8.

2D matrix of ROIs pairs showing significant rsFC differences. (A) Direct rsFC comparison of two patients' groups: 39 CH and 49 CLBP patients ($P < 0.05$, *t*-test). (B) Comparison of two controls' groups: 39 CON_{CH} and 49 CON_{CLBP}. One ROI pair [left medial orbitofrontal cortex (left ACC) – left lingual gyrus (left visual association area) (1–6)] showed rsFC differences at $P < 0.05$ level (t-test). (C) RsFC comparison across 39 CH, 49 CLBP, and 88 $CON_{CH+CLBP}$. One ROI pair [left inferior parietal cortex (left multisensory association area)–left PCC (2–4)] showed rsFC difference ($P < 0.05$, one-way ANOVA). [Color figure can be viewed at wileyonlinelibrary.com]

symptomology (BDI, STAI, HRSD), and sleep disturbances (PSQI), compared with their age- and gender-matched controls. These findings are in general agreement with previous reports of various chronic pain conditions [for reviews, see Boakye et al., 2016; Menefee et al., 2000; Neelakantan et al., 2004]. Importantly, compromised wellbeing in CH patients, such as sleep disturbance or fatigue, correlated with CT abnormalities in multisensory association area (BA39), a region that processes somatic, visual and auditory information, and multimodal posterior area (BA21). Interestingly, these psychological measures did not correlate closely with subjective pain ratings at the time data were acquired. Together, these observations indicate that compromised psychological wellbeing in chronic pain patients (CH in our study) is linked to brain structural abnormality. Therefore, effective management of chronic pain patients should include psychological evaluations. Furthermore, given the observed widespread structural and functional abnormalities observed in chronic pain patients, early intervention with a combination of psychological, pharmacological, rehabilitative, and surgical therapeutic approaches may be necessary to optimize their overall quality of life.

CT Abnormality in CH and CLBP Patients

Cortical structural abnormality has been reported in various chronic pain conditions [DaSilva et al., 2007a;

TABLE II. Cortical regions showed significantly differences in rsFC between CH and CLBP [Color table can be viewed at wileyonlinelibrary.com]

ROI	Name	Name	ROI
CH vs. CLBP (Fig. 8A)			
1	L ACC	L multimodal posterior area	5
2	L multisensory association area	L PCC	4
2	L multisensory association area	L multimodal posterior area	5
2	L multisensory association area	L visual association area	6
2	L multisensory association area	R S1 cortex	10
2	L multisensory association area	R V2 cortex	11
2	L multisensory association area	R V1 cortex	12
4	L PCC	R S1 cortex	10
5	L multimodal posterior area	R prefrontal cortex	7
5	L multimodal posterior area	R secondary sensorimotor cortex	8
7	R prefrontal cortex	R V2 cortex	11
10	R S1 cortex	R V2 cortex	11
10	R S1 cortex	R V1 cortex	12
CLBP vs. CON_{CLBP} (Fig. 7E)			
3	L premotor cortex	R V1 cortex	12
11	R V2 cortex	R V1 cortex	12

Note: Shaded ROI pairs are those shared with CH vs. CON_{CH} comparison in Fig. 6A.
Main functions of ACC (medial orbitofrontal cortex): emotional/motivational executive functions.

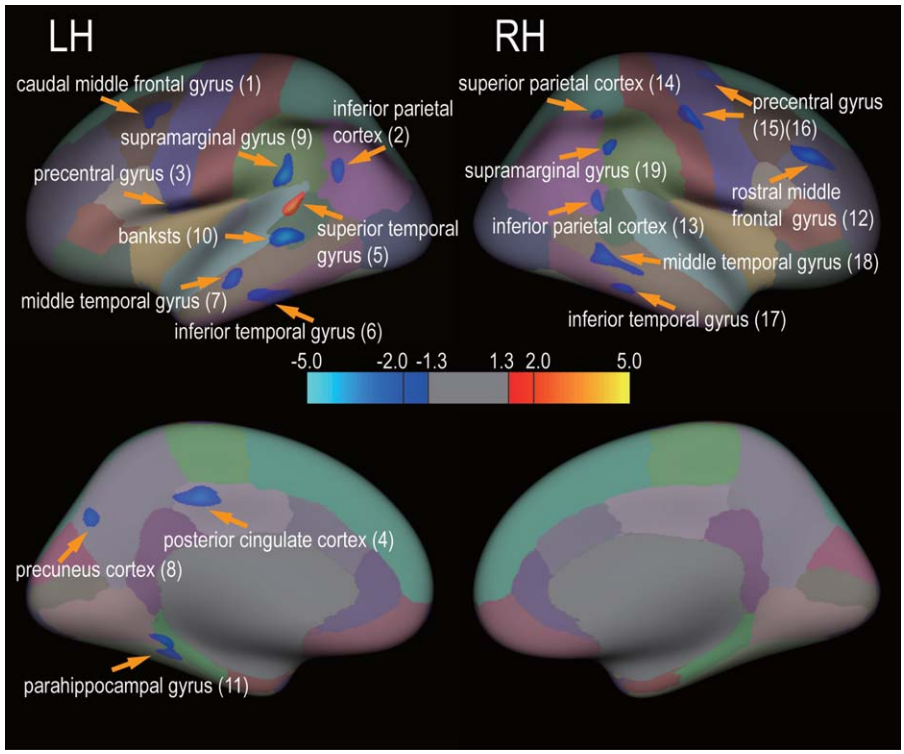

Figure 9.

Widely distributed CT abnormality in CLBP relative to CON_{CLBP} groups (49 pairs). Cortical regions that exhibited thickness abnormality are illustrated on an inflated, parcellated brain surface (color coded for 64 cortical areas, DK atlas). Light blue-blue and yellow-red colors indicate thickening and thinning, respectively. Horizontal color bar shows the range of CT abnormality (t values). Thickness abnormality (two-sample two-tailed t-test) was thresholded at $P < 0.05$ ($|t| > 1.3$), peak significant value $P < 0.01$ ($|t| > 2$), and minimal cluster size of 60 mm^2. Patches are numbered from left (L) to right (R) hemispheres.

Granziera et al., 2006]. The two most commonly used structural analysis methods are volumetric and surface based. We started our study with CT analysis, because it has been shown to be sensitive to identifying meaningful abnormalities in various disease conditions, such as migraine [Granziera et al., 2006], chronic temporomandibular pain [Moayedi et al., 2011], and irritable bowel syndrome [Blankstein et al., 2010; Davis et al., 2008].

To date, with respect to headache, controversies remain regarding the nature of CT abnormality (i.e., thickening vs. thinning) and the specific areas involved [for reviews, see May, 2009, 2011, 2013]. Here, we showed that surface-based [Lester and Liu, 2013; May, 2009] CT measurement is sufficiently sensitive to detect structural abnormality between pain (i.e., headache) and no pain conditions. In our heterogeneous CH group, we detected CT abnormality in a wide variety of regions, including premotor and S1 cortices around the central sulcus, multisensory association areas, right secondary sensorimotor cortex, and left PCC. These cortical regions are parts of different resting state networks [Damoiseaux et al., 2006], including DMN [cingulate cortices, such as PCC; Raichle, 2015a], sensorimotor (premotor, S1, and secondary sensorimotor cortices), and executive control [prefrontal and parietal regions; Seeley et al., 2007].

Numerous studies report that headache (e.g., migraine) patients have a higher risk of brain structural abnormality than their age-matched controls [Bashir et al., 2013; Hougaard et al., 2014; Kruit et al., 2010; Palm-Meinders et al., 2012]. However, the reported prevalence of subcortical structural abnormality in headache patients, including white matter lesion, varies across studies. This issue of the prevalence of subcortical white matter lesions in normal adult, CH patients, and CLBP patients motivated us to (1) quantify the prevalence of white matter lesions in CH, CON_{CH}, CLBP, and CON_{CLBP} groups, and (2) examine the relationships between CT as a function of age in both CH and CON_{CH} groups. We found overall comparable prevalence of white matter lesions in both CH patient (37%) and control (32%) groups. These numbers are higher than most of the previous reports [for reviews, see Hougaard et al., 2014; Kruit et al., 2004, 2005], which primarily employed 1.5T MRI and computed tomography images in the analysis [Eller and Goadsby, 2013; Ellerbrock et al., 2013]. We

TABLE III. Cortical regions with CLBP-associated thickness changes (Fig. 9) [Color table can be viewed at wileyonlinelibrary.com]

Index	DK atlas	BA	*t* value	Coordinates (*x*,*y*,*z*)			Size (mm^2)
° 1	L caudal middle frontal gyrus	L premotor cortex (BA6)	−2.3804	−38.2	5.7	54.5	303.44
2	L inferior parietal cortex	L multisensory association area (B39)	−2.8401	−43.0	−56.1	24.9	122.86
3	L precentral gyrus	L premotor cortex (BA6)	−2.0593	−49.2	2.6	5.1	122.33
° 4	L posterior cingulate cortex	L posterior cingulate cortex (BA31)	−2.7967	−8.8	−29.5	40.2	186.69
5	L superior temporal gyrus	L Wernicke's area (BA22)	2.7841	−63.3	−41.3	10.0	118.31
° 6	L inferior temporal gyrus	L fusiform gyrus (BA20)	−2.6886	−48.4	−37.9	−24.0	409.15
7	L middle temporal gyrus	L multimodal posterior area (BA21)	−2.3804	−57.9	−19.1	−16.0	133.30
8	L precuneus cortex	L secondary sensorimotor area (BA7)	−2.2237	−13.3	−66.5	34.0	92.34
° 9	L supramarginal gyrus	L outside BAs	−3.1154	−48.8	−44.4	26.0	192.40
° 10	L banks of the superior temporal sulcus (banksts)	L outside BAs	−3.6427	−48.1	−39.6	−0.8	197.85
11	L parahippocampal gyrus	L fusiform gyrus (BA37)	−2.0265	−26.7	−41.3	−9.8	186.60
° 12	R rostral middle frontal gyrus	R prefrontal cortex (BA9)	−3.2359	40.2	29.1	31.2	315.80
13	R inferior parietal cortex	R fusiform gyrus (BA37)	−2.4404	44.4	−48.1	13.1	86.61
14	R superior parietal cortex	R secondary sensorimotor cortex (BA7)	−2.1987	32.0	−46.7	38.4	71.52
° 15	R precentral gyrus	R primary motor cortex (M1, BA4)	−3.2219	37.3	−18.3	35.0	170.69
16	R precentral gyrus	R outside BAs	−2.7641	23.7	−12.4	53.4	131.23
17	R inferior temporal gyrus	R fusiform gyrus (BA20)	−2.6355	54.3	−41.5	−19.5	95.66
° 18	R middle temporal gyrus	R multimodal posterior area (BA21)	−2.2227	61.9	−43.4	−7.3	235.26
19	R supramarginal gyrus	R multimodal association area (BA40)	−2.0915	52.3	−43.8	35.4	98.18

Note: "°" indicates regions survived the multiple comparison corrections (Monte Carlo simulation, $P < 0.05$, FreeSurfer). Regions in left (L) or right (or R) hemispheres are highlighted by blue or red background, respectively. *x*-*y*-*z* coordinates are in MNI space. Positive and negative numbers indicate cortical thickening and thinning in CLBP patients, respectively

attribute at least part of the high detection rate of white matter lesions in our study to the use of 3T MRI FLAIR (fluid-attenuated inversion recovery) images, which have higher imaging contrast than 1.5T MRI and computed tomography images. Interestingly, we unexpectedly found high prevalence of white matter lesion in the CLBP (53%) and $CON_{CLBP,}$ (42%) groups. The mean age of the CLBP and CON_{CLBP} groups (55.4 and 55.2 years old) was approximately 12 years older than that of the CH and CON_{CH} groups (43.4 and 44.0 years old). The older mean age of the CLBP and CON_{CLBP} groups may have contributed to the high prevalence of white matter lesions, which is known to increase with age in the general population. Importantly, the degrees of CT thinning in the PCC and multimodal posterior area (engaged in visual and auditory information process) in CH patients exceeded the effect of age alone, indicating that age-related CT effects (primarily thinning) are not universal, but occur on a regional basis.

Additionally, we observed structural abnormality in specific cortical regions, such as S1, PCC, prefrontal, and visual (V1, V2, and visual association) cortices, which are consistent with regions identified in previous studies of migraine and headache patients [for reviews, see Borsook et al., 2015; May, 2013]. This provides further evidence of their involvement in CH pain. CT differences in these CH patients, however, did not correlate with the subjective self-reported pain magnitude at the time of data collection, indicating CT abnormality likely results from long-term course of insults. For example, a CT abnormality in right S1 cortex in CH is well aligned with its role in processing pain-related information [DaSilva et al., 2007a,b; Kong et al., 2013]. The constant processing of painful inputs in S1 might drive progressive cortical thickening [Kong et al., 2013]. Furthermore, the PCC is a core region of the posterior subnetwork of the DMN, which has been implicated in consciousness and memory processing via its relation to the hippocampus [Frokjaer et al., 2012; Hemington et al., 2015]. PCC thickening may reflect its constant engagement in the chronic pain experienced by CH patients. Furthermore, CT abnormality in the inferior parietal cortex (multisensory association area, BA39), which is a node of the executive control network, may be related to the multisensory association of pain with visual and auditory information, pain memory, attention, or other aspects of internal mentation in CH patents. Future longitudinal evaluation or interventional studies are needed to determine whether these structural abnormalities are causative of or consequential to CH.

Interestingly, findings in CLBP patients indicate that there are common regions (i.e., premotor cortex, PCC, multisensory association area, and prefrontal cortex) that may be associated to the chronic pain states, regardless of the specific pathology. These cortical regions exhibited similar CT abnormality in both CH and CLBP conditions. These regions indeed are widespread and belong to different functional networks. These structural abnormalities may be the underlying pathology for the multidimensional feature of chronic pain, and could be a

possible mechanism for the cognitive and emotional issues that a high percentage of chronic pain patients experience. More detailed analyses are needed to reveal these potential associations.

Correlated Structural and RsFC Abnormality

Brain regions that are engaged in processing the same peripheral inputs (e.g., pain signals) or behavior are often connected functionally at rest, as reflected by rsFC data. Correlated structural and functional connectivity abnormalities have been reported in various disease conditions [Bar et al., 2015; Jensen et al., 2013; Kregel et al., 2015; May, 2009]. Building upon this concept, we parcellated cortical regions showing structural abnormality, and regrouped them into functionally relevant networks by measuring the inter-regional correlation strength of their rsfMRI signals. We used the correlation analysis of the low-frequency fluctuations (0.01–0.08 Hz) of rsfMRI signals to evaluate intrinsic inter-regional rsFC [for reviews of mechanism and applications, see [Raichle, 2015b; Ramani, 2015; Zhang and Raichle, 2010]. In line with previous observations indicating coordinated activity during the processing of nociceptive heat inputs in non-human primates [Wang et al., 2013], we identified strong rsFC between premotor and S1 (areas 1, 2, 3a,b) cortices in controls. This finding indicates that sensory and motor regions do exhibit strong intrinsic functional connectivity. The strong connection between premotor and S1 cortices was weakened in CH patients suggesting that they may have some form of compromised communication in sensorymotor networks. Pairwise rsFC comparisons between the CH patients and their controls revealed only four ROI pairs with significantly enhanced connectivity. Within these functional circuits, the left inferior parietal cortex, where multisensory association area [BA39, engaged in somatosensory (includes pain), visual and auditory information] resides, serves as a core hub connecting S1 cortex (right postcentral gyrus), left PCC, left multimodal posterior area (BA21), and left visual association area. These findings indicate that rsFCs among multisensory, sensorimotor, sensory association areas, cingulate, multimodal posterior and prefrontal regions are disrupted in CH patients.

RsFC Abnormality Differ Across Chronic Pain Conditions

Given the complexity of chronic pain experiences, it is possible that some brain regions are involved in encoding pathology-specific information (i.e., head vs. lower back) whereas others are responsible for encoding different information, such as pain quality [Apkarian et al., 2005, 2009, 2013; Kregel et al., 2015]. When we compared abnormalities in inter-regional rsFC between CLBP and their controls, only two ROI pairs, between the left premotor and right V1 cortices, and V1 and V2 visual cortices in the right hemisphere, showed rsFC difference (Table II). The observations of no overlap abnormality in rsFC between CH versus CON_{CH} and CLBP versus $CON_{CLBP,}$ but shared rsFC disturbance in CH versus CLBP, indicate that rsFC strengthening in the four core ROIs likely relates to the specific pathology of CH versus CLBP conditions. It also suggests that neural circuits involved in CLBP differ from those involved in CH. Furthermore, only one ROI pair of multisensory association area of the inferior parietal cortex and PCC showed significantly different rsFC when we compared all three groups (CH, CLBP, and CON). Both of these regions are core nodes of DMN and executive control networks.

RsFC differences between CH and CLBP patients indicate that connectivity abnormalities are specific to local cortical regions and strongly relate to the underlying pathology of the chronic pain condition. However, we speculate that age and gender differences between these groups likely resulted in a loss of statistical power in detecting differences in other ROI pairs. Fine-scale functional organization differences within a single functional region and the size of the ROI seeds likely influence rsFC measures. We think that the use of ROI seeds with a radius of 10 mm in our rsFC analysis improved our ability to differentiate between the groups, at least in those regions showing CT abnormality in CH patients [Eickhoff et al., 2006]. The detection of structural and functional abnormality in multiple sites of the same large region (e.g., multisensory association area) provides evidence for the existence of functionally distinct subregions. It is possible that the size of the ROI likely captured rsfMRI signal fluctuations originating from a cortical region containing more functionally homogenous neurons. It also likely contributes to the discrepancy in what brain regions are found to be involved in mediating abnormality in specific pain related multi-dimensional experiences. Finally, rsFC differences between CH and CLBP patients indicate that connectivity abnormalities are specific to local cortical regions and strongly related to the underlying pathology of the chronic pain condition.

CONCLUSION

We observed compromised psychological wellbeing and widespread CT abnormality in CH patients. CT abnormality was associated with rsFC alterations (i.e., left multisensory association area–right S1 cortex, left multisensory association area–left PCC, left multisensory association area–left multimodal posterior area, and left multisensory association area–left visual association area). The CT abnormality shared some common features with those of CLBP, whereas rsFC abnormality observed in CH patients differed from that observed in CLBP patients. The functional connectivity between PCC and multisensory association regions was the most robust measure that could differentiate the three groups of CH, CLBP, and CON.

ACKNOWLEDGEMENTS

We thank Dr. Yong Zhu, Dr. Qingji Zhang, and Mrs. Youyun Li for their assistance with data collection.

REFERENCES

Apkarian AV (2010): Human brain imaging studies of chronic pain: Translational opportunities. In: Kruger L, Light AR, editors. Translational Pain Research: From Mouse to Man. Boca Raton, FL: CRC Press/Taylor & Francis.

Apkarian AV, Bushnell MC, Treede RD, Zubieta JK (2005): Human brain mechanisms of pain perception and regulation in health and disease. Eur J Pain 9:463–484.

Apkarian AV, Baliki MN, Geha PY (2009): Towards a theory of chronic pain. Prog Neurobiol 87:81–97.

Apkarian AV, Baliki MN, Farmer MA (2013): Predicting transition to chronic pain. Curr Opin Neurol 26:360–367.

Bar KJ, de la Cruz F, Berger S, Schultz CC, Wagner G (2015): Structural and functional differences in the cingulate cortex relate to disease severity in anorexia nervosa. J Psychiatry Neurosci 40:269–279.

Bashir A, Lipton RB, Ashina S, Ashina M (2013): Migraine and structural changes in the brain: A systematic review and meta-analysis. Neurology 81:1260–1268.

Beck AT, Alford BA (2009): Depression: Causes and Treatment, 2nd ed. Philadelphia: University of Pennsylvania Press.

Biswal B, Yetkin FZ, Haughton VM, Hyde JS (1995): Functional connectivity in the motor cortex of resting human brain using echo-planar MRI. Magn Reson Med 34:537–541.

Blackburn-Munro G, Blackburn-Munro RE (2001): Chronic pain, chronic stress and depression: Coincidence or consequence?. J Neuroendocrinol 13:1009–1023.

Blankstein U, Chen J, Diamant NE, Davis KD (2010): Altered brain structure in irritable bowel syndrome: Potential contributions of pre-existing and disease-driven factors. Gastroenterology 138:1783–1789.

Boakye PA, Olechowski C, Rashiq S, Verrier MJ, Kerr B, Witmans M, Baker G, Joyce A, Dick BD (2016): A critical review of neurobiological factors involved in the interactions between chronic Pain, depression, and sleep disruption. Clin J Pain 32: 327–336.

Borsook D, Becerra L, Burstein R (2015): Imaging Migraine. Philadelphia, Baltimore, New York, London, Buenos Aires, Hong Kong, Sydney, Tokyo: Wolters Kluwer.

Buysse DJ, Reynolds CF, III, Monk TH, Berman SR, Kupfer DJ (1989): The Pittsburgh Sleep Quality Index: A new instrument for psychiatric practice and research. Psychiatry Res 28: 193–213.

Ceko M, Seminowicz DA, Bushnell MC, Olausson HW (2013): Anatomical and functional enhancements of the insula after loss of large primary somatosensory fibers. Cereb Cortex 23: 2017–2024.

Chen LM, Dillenburger CD, Wang F, Tang CH (2011): Differential fMRI activation to noxious heat and tactile stimuli in parasylvian areas of new world monkeys. Pain 153:158–169.

Chou R, Qaseem A, Snow V, Casey D, Cross JT, Jr., Shekelle P, Owens DK, Clinical Efficacy Assessment Subcommittee of the American College of Physicians, American College of Physicians, American Pain Society Low Back Pain Guidelines Physicians (2007): Diagnosis and treatment of low back pain: A joint clinical practice guideline from the American College of Physicians and the American Pain Society. Ann Intern Med 147: 478–491.

Damoiseaux JS, Rombouts SA, Barkhof F, Scheltens P, Stam CJ, Smith SM, Beckmann CF (2006): Consistent resting-state networks across healthy subjects. Proc Natl Acad Sci U S A 103: 13848–13853.

DaSilva AF, Granziera C, Snyder J, Hadjikhani N (2007a): Thickening in the somatosensory cortex of patients with migraine. Neurology 69:1990–1995.

DaSilva AF, Granziera C, Tuch DS, Snyder J, Vincent M, Hadjikhani N (2007b): Interictal alterations of the trigeminal somatosensory pathway and periaqueductal gray matter in migraine. Neuroreport 18:301–305.

Davis KD, Moayedi M (2013): Central mechanisms of pain revealed through functional and structural MRI. J Neuroimmune Pharmacol 8:518–534.

Davis KD, Pope G, Chen J, Kwan CL, Crawley AP, Diamant NE (2008): Cortical thinning in IBS: Implications for homeostatic, attention, and pain processing. Neurology 70:153–154.

Desikan RS, Segonne F, Fischl B, Quinn BT, Dickerson BC, Blacker D, Buckner RL, Dale AM, Maguire RP, Hyman BT, Albert MS, Killiany RJ (2006): An automated labeling system for subdividing the human cerebral cortex on MRI scans into gyral based regions of interest. NeuroImage 31:968–980.

Eickhoff SB, Heim S, Zilles K, Amunts K (2006): Testing anatomically specified hypotheses in functional imaging using cytoarchitectonic maps. NeuroImage 32:570–582.

Eller M, Goadsby PJ (2013): MRI in headache. Expert Rev Neurother 13:263–273.

Ellerbrock I, Engel AK, May A (2013): Microstructural and network abnormalities in headache. Curr Opin Neurol 26:353–359.

Emerson NM, Zeidan F, Lobanov OV, Hadsel MS, Martucci KT, Quevedo AS, Starr CJ, Nahman-Averbuch H, Weissman-Fogel I, Granovsky Y, Yarnitsky D, Coghill RC (2014): Pain sensitivity is inversely related to regional gray matter density in the brain. Pain 155:566–573.

Fasick V, Spengler RN, Samankan S, Nader ND, Ignatowski TA (2015): The hippocampus and TNF: Common links between chronic pain and depression. Neurosci Biobehav Rev 53:139–159.

Fox MD, Greicius M (2010): Clinical applications of resting state functional connectivity. Front Syst Neurosci 4:19.

Freund W, Wunderlich AP, Stuber G, Mayer F, Steffen P, Mentzel M, Weber F, Schmitz B (2010): Different activation of opercular and posterior cingulate cortex (PCC) in patients with complex regional pain syndrome (CRPS I) compared with healthy controls during perception of electrically induced pain: A functional MRI study. Clin J Pain 26:339–347.

Frokjaer JB, Bouwense SA, Olesen SS, Lundager FH, Eskildsen SF, van Goor H, Wilder-Smith OH, Drewes AM (2012): Reduced cortical thickness of brain areas involved in pain processing in patients with chronic pancreatitis. Clin Gastroenterol Hepatol 10:434–438.

Granziera C, DaSilva AF, Snyder J, Tuch DS, Hadjikhani N (2006): Anatomical alterations of the visual motion processing network in migraine with and without aura. PLoS Med 3:e402.

Hamilton M (1960): A rating scale for depression. J Neurol Neurosurg Psychiatry 23:56–62.

Headache Classification Committee of the International Headache Society (IHS) (2013): The international classification of headache disorders, 3rd edition (beta version). Cephalalgia 33: 629–808.

Hemington KS, Wu Q, Kucyi A, Inman RD, Davis KD (2015): Abnormal cross-network functional connectivity in chronic pain and its association with clinical symptoms. Brain Struct Funct 21:4203–4219.

Hougaard A, Amin FM, Ashina M (2014): Migraine and structural abnormalities in the brain. Curr Opin Neurol 27:309–314.

Hubbard CS, Khan SA, Keaser ML, Mathur VA, Goyal M, Seminowicz DA (2014): Altered brain structure and function correlate with disease severity and pain catastrophizing in migraine patients. eNeuro 1:e2014.

Ichesco E, Puiu T, Hampson JP, Kairys AE, Clauw DJ, Harte SE, Peltier SJ, Harris RE, Schmidt-Wilcke T (2016): Altered fMRI resting-state connectivity in individuals with fibromyalgia on acute pain stimulation. Eur J Pain 20:1079–1089.

Jensen KB, Srinivasan P, Spaeth R, Tan Y, Kosek E, Petzke F, Carville S, Fransson P, Marcus H, Williams SC, Choy E, Vitton O, Gracely R, Ingvar M, Kong J (2013): Overlapping structural and functional brain changes in patients with long-term exposure to fibromyalgia pain. Arthritis Rheum 65:3293–3303.

Kim JY, Kim SH, Seo J, Kim SH, Han SW, Nam EJ, Kim SK, Lee HJ, Lee SJ, Kim YT, Chang Y (2013): Increased power spectral density in resting-state pain-related brain networks in fibromyalgia. Pain 154:1792–1797.

Kong J, Spaeth RB, Wey HY, Cheetham A, Cook AH, Jensen K, Tan Y, Liu H, Wang D, Loggia ML, Napadow V, Smoller JW, Wasan AD, Gollub RL (2013): S1 is associated with chronic low back pain: A functional and structural MRI study. Mol Pain 9:43.

Kregel J, Meeus M, Malfliet A, Dolphens M, Danneels L, Nijs J, Cagnie B (2015): Structural and functional brain abnormalities in chronic low back pain: A systematic review. Semin Arthritis Rheum 45:229–237.

Kruit MC, van Buchem MA, Hofman PA, Bakkers JT, Terwindt GM, Ferrari MD, Launer LJ (2004): Migraine as a risk factor for subclinical brain lesions. jama 291:427–434.

Kruit MC, Launer LJ, van Buchem MA, Terwindt GM, Ferrari MD (2005): MRI findings in migraine. Rev Neurol (Paris) 161: 661–665.

Kruit MC, van Buchem MA, Launer LJ, Terwindt GM, Ferrari MD (2010): Migraine is associated with an increased risk of deep white matter lesions, subclinical posterior circulation infarcts and brain iron accumulation: The population-based MRI CAMERA study. Cephalalgia 30:129–136.

Lester MS, Liu BP (2013): Imaging in the evaluation of headache. Med Clin North Am 97:243–265.

Mansour AR, Farmer MA, Baliki MN, Apkarian AV (2014): Chronic pain: The role of learning and brain plasticity. Restor Neurol Neurosci 32:129–139.

May A (2009): New insights into headache: An update on functional and structural imaging findings. Nat Rev Neurol 5:199–209.

May A (2011): Structural brain imaging: A window into chronic pain. Neuroscientist 17:209–220.

May A (2013): Pearls and pitfalls: Neuroimaging in headache. Cephalalgia 33:554–565.

Menefee LA, Cohen MJ, Anderson WR, Doghramji K, Frank ED, Lee H (2000): Sleep disturbance and nonmalignant chronic pain: A comprehensive review of the literature. Pain Med 1:156–172.

Mishra A, Rogers BP, Chen LM, Gore JC (2014): Functional connectivity-based parcellation of amygdala using self-organized mapping: A data driven approach. Hum Brain Mapp 35:1247–1260.

Moayedi M, Davis KD (2013): Theories of pain: From specificity to gate control. J Neurophysiol 109:5–12.

Moayedi M, Weissman-Fogel I, Crawley AP, Goldberg MB, Freeman BV, Tenenbaum HC, Davis KD (2011): Contribution of chronic pain and neuroticism to abnormal forebrain gray matter in patients with temporomandibular disorder. NeuroImage 55:277–286.

Neelakantan D, Omojole F, Clark TJ, Gupta JK, Khan KS (2004): Quality of life instruments in studies of chronic pelvic pain: A systematic review. J Obstet Gynaecol 24:851–858.

Nelson SM, Cohen AL, Power JD, Wig GS, Miezin FM, Wheeler ME, Velanova K, Donaldson DI, Phillips JS, Schlaggar BL, Petersen SE (2010): A parcellation scheme for human left lateral parietal cortex. Neuron 67:156–170.

Palm-Meinders IH, Koppen H, Terwindt GM, Launer LJ, Konishi J, Moonen JM, Bakkers JT, Hofman PA, van Lew B, Middelkoop HA, van Buchem MA, Ferrari MD, Kruit MC (2012): Structural brain changes in migraine. jama 308:1889–1897.

Raichle ME (2015a): The brain's default mode network. Annu Rev Neurosci 38:433–447.

Raichle ME (2015b): The restless brain: How intrinsic activity organizes brain function. Philos Trans R Soc Lond B Biol Sci 370:20140172.

Ramani R (2015): Connectivity. Curr Opin Anaesthesiol 28: 498–504.

Seeley WW, Menon V, Schatzberg AF, Keller J, Glover GH, Kenna H, Reiss AL, Greicius MD (2007): Dissociable intrinsic connectivity networks for salience processing and executive control. J Neurosci 27:2349–2356.

Sheline YI, Raichle ME (2013): Resting state functional connectivity in preclinical Alzheimer's disease. Biol Psychiatry 74:340–347.

Takekawa KS, Goncalves JS, Moriguchi CS, Coury HJ, Sato Tde O (2015): Can a self-administered questionnaire identify workers with chronic or recurring low back pain?. Ind Health 53:340–345.

Tilton SR (2008): Review of the state-trait anxiety inventory. NewsNotes 48:1–3.

Vincent JL, Patel GH, Fox MD, Snyder AZ, Baker JT, Van Essen DC, Zempel JM, Snyder LH, Corbetta M, Raichle ME (2007): Intrinsic functional architecture in the anaesthetized monkey brain. Nature 447:83–86.

Wang Z, Chen LM, Negyessy L, Friedman RM, Mishra A, Gore JC, Roe AW (2013): The relationship of anatomical and functional connectivity to resting-state connectivity in primate somatosensory cortex. Neuron 78:1116–1126.

Ware JE, Sherbourne CD (1992): The MOS 36-Item Short-Form Health Survey (SF-36): I. conceptual framework and item selection. Med Care 30:473–483.

Williams JBW (1988): A structured interview guide for the Hamilton Depression Rating Scale. Arch Gen Psychiatry 45:742–747.

Xia M, Wang J, He Y (2013): BrainNet Viewer: A network visualization yool for human brain connectomics. PLoS ONE 8:e68910.

Yi H, Ji X, Wei X, Chen Z, Wang X, Zhu X, Zhang W, Chen J, Zhang D, Li M (2012): Reliability and validity of simplified Chinese version of Roland-Morris questionnaire in evaluating rural and urban patients with low back pain. PLoS One 7:e30807.

Zhang D, Raichle ME (2010): Disease and the brain's dark energy. Nat Rev Neurol 6:15–28.

Zhang D, Snyder AZ, Shimony JS, Fox MD, Raichle ME (2010): Noninvasive functional and structural connectivity mapping of the human thalamocortical system. Cereb Cortex 20:1187–1194.

Zheng Z, Xiao Z, Shi X, Ding M, Di W, Qi W, Zhang A, Fang Y (2014): White matter lesions in chronic migraine with medication overuse headache: A cross-sectional MRI study. J Neurol 261:784–790.